Biosensors and Bioelectronics 186 (2021) 113279

Contents lists available at ScienceDirect

Biosensors and Bioelectronics

journal homepage: www.elsevier.com/locate/bios

Aptamer-based lateral flow assay on-site biosensors

Lei Huang [a], Shulin Tian [a], Wenhao Zhao [a], Ke Liu [a,*], Xing Ma [b,c,**], Jinhong Guo [d,***]

[a] School of Automation Engineering, University of Electronic Science and Technology of China, Chengdu, 611731, China
[b] School of Materials Science and Engineering, Harbin Institute of Technology (Shenzhen), Shenzhen, 518055, China
[c] Shenzhen Bay Laboratory, No.9 Duxue Road, Shenzhen, 518055, China
[d] School of Information and Communication Engineering, University of Electronic Science and Technology of China, Chengdu, 611731, China

ARTICLE INFO

Keywords:
Aptamer
Biosensor
Lateral flow assay
On-site detection

ABSTRACT

The lateral flow assay (LFA) is a widely used paper-based on-site biosensor that can detect target analytes and obtain test results in several minutes. Generally, antibodies are utilized as the biorecognition molecules in the LFA. However, antibodies selected using an *in vivo* process not only may risk killing the animal hosts and causing errors between different batches but also their range is restricted by the refrigerated conditions used to store them. To avoid these limitations, aptamers screened by an *in vitro* process have been studied as biorecognition molecules in LFAs. Based on the sandwich or competitive format, the aptamer-based LFA can accomplish on-site detection of target analytes. Since aptamers have a distinctive ability to undergo conformational changes, the adsorption–desorption format has also been exploited to detect target analytes in aptamer-based LFAs. This paper reviews developments in aptamer-based LFAs in the last three years for the detection of target analytes. Three formats of aptamer-based LFAs, i.e., sandwich, competitive, and adsorption–desorption, are described in detail. Based on these formats, signal amplification strategies and multiplexed detection are discussed in order to provide an overview of aptamer-based LFAs for on-site detection of target analytes. In addition, the potential commercialization and future perspectives of aptamer-based LFAs for rapid detection of SARS-CoV-2 are given to support the COVID-19 pandemic.

1. Introduction

The lateral flow assay (LFA) is a widely used paper-based on-site biosensor that can detect target analytes in a given sample (usually dozens of milliliters) and obtain test results in several minutes without the need for well-trained personnel to operate expensive and sophisticated instrumentation (Bahadir and Sezginturk, 2016). Therefore, it has garnered considerable interest among researchers for its advantages of easy operation, low cost, and rapid detection, making it favorable for point-of-care testing (Bahadir and Sezginturk, 2016; Banerjee and Jaiswal, 2018; Gong et al., 2017; Kim et al., 2019a; Quesada-Gonzalez and Merkoci, 2015; Zhao et al., 2018). Since the successful launch of the first commercial product for urine-based pregnancy detection, the LFA has been widely applied in diverse fields, including food safety, clinical analysis, and environmental monitoring (Huang et al., 2016; Soh et al., 2020; Van-Thuan et al., 2020; Wang et al., 2016).

Conventionally, the LFA consists of a sample pad, conjugate pad, nitrocellulose (NC) membrane, absorbent pad, and backing card, where the first four parts are assembled on the backing card with appropriate overlap. The sample pad is utilized to load the sample of interest, which then flows to other parts of the LFA via capillary force. The conjugate pad pre-deposits the labeled biorecognition molecule that binds to the target analyte. The NC membrane is employed to pre-immobilize the capture molecule and control molecule as the test line (TL) and control line (CL), respectively. The absorbent pad provides the capillary force and prevents backflow of the loaded sample (Huang et al., 2020).

Generally, antibodies are utilized as the biorecognition molecules in LFAs (Chen et al., 2016; Sun et al., 2018; Yan et al., 2019; Zhan et al., 2019; Zhang et al., 2018a). Although antibodies with high sensitivity and specificity have proved highly successful, they are still subject to easy denaturation and the inability to renature, making them unstable and further limiting their applications. Additionally, antibodies selected using an *in vivo* process not only risk killing the animal hosts and causing errors between different batches but also their range is restricted by the

* Corresponding author.
** Corresponding author. School of Materials Science and Engineering, Harbin Institute of Technology (Shenzhen), Shenzhen, 518055, China.
*** Corresponding author.
E-mail addresses: liuke@uestc.edu.cn (K. Liu), maxing@hit.edu.cn (X. Ma), guojinhong@uestc.edu.cn (J. Guo).

https://doi.org/10.1016/j.bios.2021.113279
Received 1 February 2021; Received in revised form 19 March 2021; Accepted 20 April 2021
Available online 24 April 2021

refrigerated conditions used to store them (Farka et al., 2017; Kuhn et al., 2016; Reid et al., 2020). Nowadays, aptamers that are screened by an *in vitro* iterative process called systematic evolution of ligands by exponential enrichment (SELEX) have been exploited to overcome these limitations (Schüling et al., 2018).

Aptamers are single-stranded DNA (ssDNA) or RNA molecules that can bind to proteins or other small molecules with high affinity and specificity (Chen and Yang, 2015; Dhiman et al., 2017; Huang et al., 2015; Minagawa et al., 2017; Rasoulinejad and Gargari, 2016; Reinemann et al., 2016; Seok et al., 2015; Wu et al., 2019; Yin et al., 2015). Due to their inherent nature as nucleic acids, aptamers are highly stable and capable of recovering their natural conformation following denaturation, making them sufficiently flexible to adapt to different assay formats (Amraee et al., 2017; Hyeon et al., 2012; Kim et al., 2016; Ozalp et al., 2015; Raston and Gu, 2015; Van-Thuan et al., 2017). While the process of selecting aptamers may be expensive, once aptamers are screened, they can be synthesized with high reproducibility and purity, leading to the cost of aptamers being remarkably lower than that of antibodies (Chung et al., 2015; Diaz-Amaya et al., 2019; Gopinath et al., 2016; Wang et al., 2019; Wu et al., 2015; Yu et al., 2017). Recently, aptamers have been thoroughly studied as biorecognition molecules for various LFAs (Bruno et al., 2012; Fang et al., 2014; Liu et al., 2009; Mao et al., 2009; Raston et al., 2017; Shim et al., 2014; Wang et al., 2011; Xu et al., 2009; Zhou et al., 2016). A comparison of antibody-based LFAs and aptamer-based LFAs is listed in Table 1.

According to a latest research, the global aptamer market was valued nearly $916 million in 2020 and is anticipated to reach about $1827 million by 2025, with a compound annual growth rate (CAGR) of 14.8% (https://www.marketresearch.com/360iResearch-v4164/Aptamers-Research-Type-DNA-based-13972867/). This growth is attributable to the rapid advancements in technology for screening aptamers and increasing attention to aptamers by numerous researchers. Although the most of aptamer market is based on the aptamer synthesis, there is no doubt that aptamer-based LFAs are demonstrating their merits and potential for on-site detection.

Based on the sandwich or competitive format, the aptamer-based LFA can accomplish on-site detection of target analytes. The sandwich format is more suitable for analytes with multiple epitopes, whereas the competitive format is preferred for analytes with only one epitope. In the sandwich format, the analyte in the sample initially reacts with the labeled aptamer and is then captured by the capture molecule to form a sandwich on the TL. In the competitive format, the analyte and the capture molecule compete with each other to react with the labeled aptamer. Regardless of whether the sample contains the analyte or not, the labeled aptamer molecule can eventually be captured by the control molecule on the CL, indicating the proper functioning of the aptamer-based LFA. Since aptamers have a distinctive ability to undergo conformational changes, the adsorption–desorption format has also been exploited to detect target analytes in aptamer-based LFAs. This format relies on the adsorption of aptamer onto the surface of the label and the subsequent desorption of aptamer from the labeled aptamer (Jauset-Rubio et al., 2017). The schematic picture of sandwich, competitive, and adsorption–desorption formats for aptamer-based LFAs is illustrated in Scheme 1.

This paper reviews developments in aptamer-based LFA in the last three years for the detection of target analytes. Three formats of aptamer-based LFAs, i.e., sandwich, competitive, and adsorption–desorption, are described in detail. Based on these formats, signal amplification strategies, multiplexed detection, and future perspectives are discussed in order to provide an overview of aptamer-based LFAs for on-site detection of target analytes.

2. Sandwich format for aptamer-based LFAs

The sandwich format for aptamer-based LFAs is the most frequently applied format for the detection of analytes with multiple epitopes that can bind to a pair of aptamers or to a combination of aptamers and antibodies. For enhanced sensitivity, different signal amplification strategies have been exploited. In addition, researchers have devoted considerable efforts to accomplishing multiplexed detection using the aptamer-based LFA sandwich format. A summary of sandwich format for aptamer-based LFAs is listed in Table 2.

2.1. Sandwich LFA with a pair of aptamers

In a typical sandwich LFA employing a pair of aptamers, a primary aptamer is immobilized on the TL as capture probe and a labeled biotinylated secondary aptamer is dispersed on the conjugate pad as the detection probe. Streptavidin is immobilized on the CL as the control probe. When the analyte is applied to the sample pad, it initially binds to the labeled secondary aptamer and is then captured by the primary aptamer, generating a sandwich on the TL. The excess labeled biotinylated secondary aptamer can be captured by the streptavidin on the CL *via* affinity reaction between streptavidin and biotin. Therefore, the appearance of two characteristic bands on the TL and CL indicates a positive result, while a single characteristic band on the CL indicates a negative result.

Recently, Shin et al. designed a sandwich LFA employing a pair of aptamers for the detection of *Vibrio fischeri* (*V. fischeri*) in 10 min, as shown in Fig. 1(a) (Shin et al., 2018). In this assay, the *V. fischeri* cell aptamer (VFCA) pair, VFCA-02 and VFCA-03, were successfully screened by Cell-SELEX. Carboxyl-modified gold nanoparticles (AuNPs) were then applied to conjugate with biotinylated VFCA-02 aptamers to form AuNP–VFCA-02 detection probes, which were deposited on the conjugate pad. At the same time, VFCA-03 aptamers and streptavidin were immobilized on the TL and CL as capture and control probes, respectively. When a positive sample was applied to the sample pad, *V. fischeri* initially bound to the AuNP–VFCA-02 detection probes to form AuNP–VFCA-02/*V. fischeri* complexes, which were further captured by the VFCA-03 aptamers on the TL, forming sandwich complexes (AuNP–VFCA-02/*V. fischeri*/VFCA-03) with a characteristic red band. When a negative sample was applied, no sandwich complexes were formed on the TL. Regardless of whether *V. fischeri* was present in the sample or not, excess biotinylated AuNP–VFCA-02 detection probes were captured by the streptavidin on the CL *via* streptavidin–biotin affinity reaction, evidencing that the LFA was working properly. Finally, a reader was applied to detect *V. fischeri* with a linear range of 4×10^1 to 4×10^5 colony-forming units (CFUs)/mL. Using the same principle described above, Li et al. developed a sandwich LFA to detect rongalite in 15 min (Li et al., 2018). Specifically, a streptavidin-biotinylated primary aptamer A09 and a biotinylated secondary aptamer B09 conjugated with AuNPs (AuNP–B09) were designed as capture and detection probes, respectively. Streptavidin was also immobilized on the CL as the control probe in order to capture excess biotinylated AuNP–B09 detection probes. The limit of detection (LOD) obtained with the naked eye for rongalite in food samples was 1 μg mL^{-1}.

Sometimes, ssDNA complementary to the secondary aptamer is immobilized on the CL to capture the detection probe. Lee et al.

Table 1
A comparison of antibody-based LFAs and aptamer-based LFAs.

Comparison	Specificity	Sensitivity	Tunability	Reproducibility	Commercialization
Antibody-based LFAs	High	High	Poor	Poor	High degree
Aptamer-based LFAs	High	High	Flexible	High	Low degree

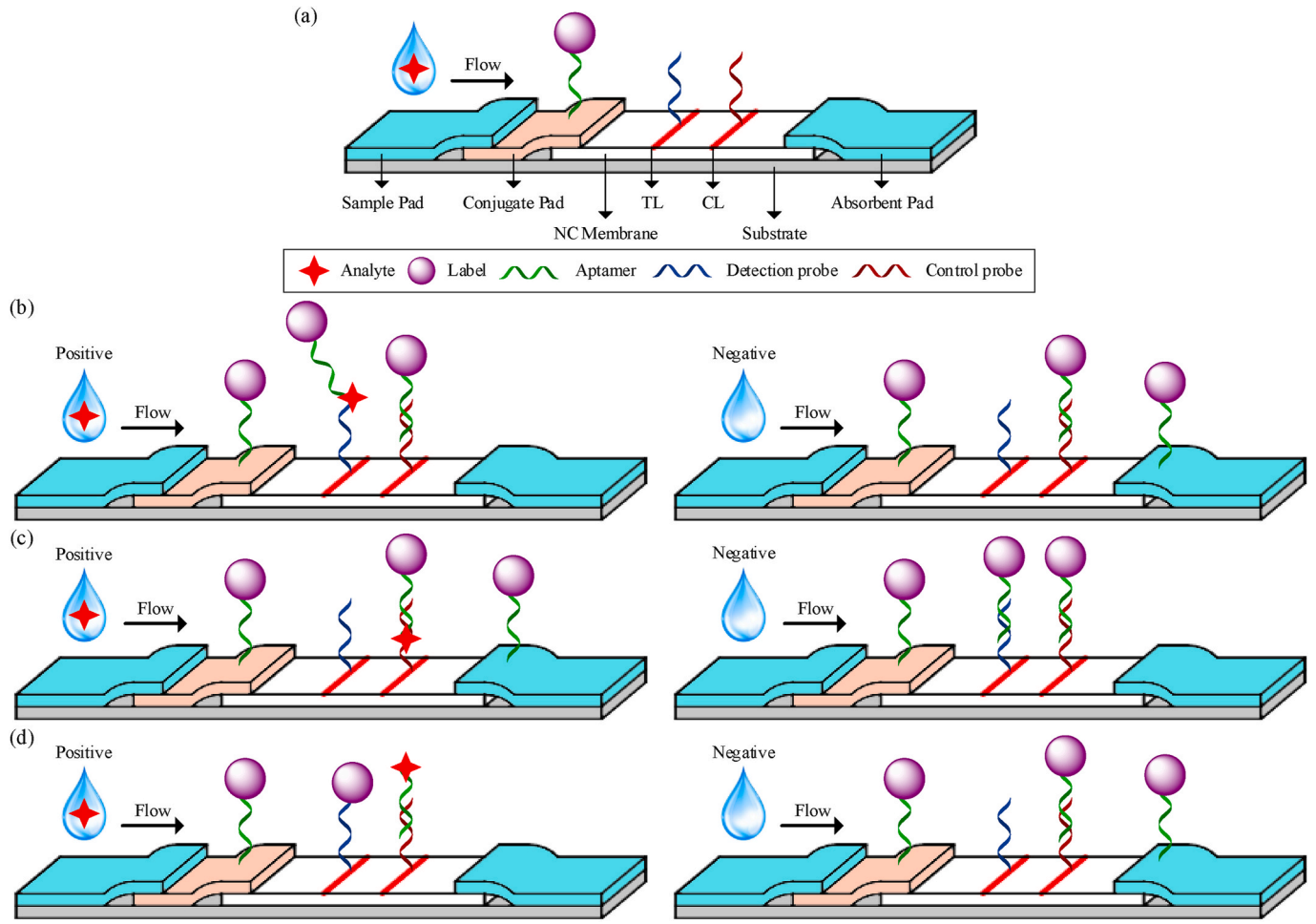

Scheme 1. Schematic diagram of aptamer-based LFA (a); sandwich (b), competitive (c), and adsorption–desorption (d) formats of aptamer-based LFAs.

presented a sandwich LFA using ssDNA on the CL for the detection of odontogenic ameloblast-associated protein (ODAM) (Lee et al., 2019). As shown in Fig. 1(b), primary aptamer (OD64) immobilized on the TL and secondary aptamer (OD35) conjugated with AuNPs were selected as capture and detection probes, respectively. Complementary ssDNA for OD35 was immobilized on the CL as the control probe. The LODs obtained with the naked eye were 8.32 nM in buffer and 14.59 nM in saliva samples. Similarly, his team proposed another sandwich LFA using a cognate pair of aptamers, primary aptamer (J_3APT) and secondary aptamer (JH_4APT), for the detection of H5N2 virus particles (Kim et al., 2019b). The LODs detected with the naked eye were 6×10^5 50% egg infection dose (EID_{50}/mL) and 1.2×10^6 EID_{50}/mL in buffer and duck feces, respectively. By using ImageJ software, the LODs obtained were 1.27×10^5 EID_{50}/mL and 2.09×10^5 EID_{50}/mL in buffer and duck feces, respectively.

In addition to AuNPs, copper oxide nanoparticles (CuO NPs) and upconversion nanoparticles (UCNPs) have been applied in the sandwich format of aptamer-based LFAs. For example, Yang et al. explored a sandwich LFA using CuO NPs as the label for the detection of HPV16-DNA in 20 min (Yang et al., 2019). As shown in Fig. 1(c), streptavidin-coated CuO NPs were adopted to react with biotin-modified capture DNA to form CuO–DNA detection probes. At the same time, streptavidin-biotinylated test DNA (tDNA) and control DNA (cDNA) were immobilized on the TL and CL as the capture and control probes, respectively. On adding the mixture of target HPV16-DNA and CuO–DNA detection probes, a CuO–DNA/HPV16-DNA/tDNA sandwich was formed on the TL with a brown band. The excess CuO–DNA detection probes were captured by cDNA on the CL, forming a second brown band. The detection range achieved with a reader was 5–100 nM, with an LOD of 1.0 nM. Recently, Ali et al. evaluated a sandwich LFA using UCNPs ($NaYF_4$:Yb,Er) as the label for the detection of visceral adipose tissue-derived serpin (Vaspin) (Ali et al., 2020). A pair of cognate aptamers (streptavidin-biotinylated primary aptamer immobilized on the TL and secondary aptamer conjugated with UCNP) were applied as detection and capture probes, respectively. Streptavidin-biotinylated control aptamer was immobilized on the CL to capture the secondary aptamer. The fluorescent intensities of the UCNPs on the TL and CL were measured using a smartphone. The linear range and LOD for Vaspin were 0.1–55 ng mL^{-1} and 39 pg mL^{-1}, respectively.

Although the sandwich format can provide reliable results for diverse targets, the detection range of the sandwich format is often limited by the hook effect, which refers to the phenomenon of false negatives because of inappropriate ratios of aptamers and analytes. To address this problem, Gao et al. investigated a three-line sandwich LFA for the detection of thrombin, as shown in Fig. 1(d) (Gao et al., 2019). A thrombin line (TBL) was added between the TL (streptavidin–tDNA) and CL (streptavidin–cDNA). At the same time, deoxyadenosine triphosphate (DATP) was applied as a sealant between the AuNPs and the thrombin aptamer to form AuNP–Apt detection probes. After the pre-incubation of the thrombin and AuNP–Apt detection probes, the mixture was dropped onto the sample pad. At low levels of thrombin, a small number of AuNP–Apt/thrombin complexes were captured by the tDNA on the TL, generating a weak red band, while the abundant AuNP–Apt detection probes were captured by thrombin on the TBL and formed a strong red band. Comparatively fewer AuNP–Apt detection probes were captured by cDNA on the CL, resulting in a red band slightly

Table 2
A summary of sandwich format for aptamer-based LFAs.

Target analyte	Detection probe	TL	CL	LOD	Reference
V. fischeri	AuNP–VFCA-02-biotin	VFCA-03	Streptavidin	NA	Shin et al. (2018)
Rongalite	AuNP–B09-biotin	Streptavidin–biotin-A09	Streptavidin	1 μg mL^{-1}	Li et al. (2018)
ODAM	AuNP–OD35	OD64	ssDNA	8.32 nM in buffer and 14.59 nM in saliva	Lee et al. (2019)
H5N2	AuNP–JH_4APT-poly T	Streptavidin–biotin-J_3APT	Streptavidin–biotin-poly A	1.27×10^5 EID_{50}/mL in buffer and 2.09×10^5 EID_{50}/mL in duck feces	Kim et al. (2019b)
Cortisol	AuNP–DNA	Streptavidin–biotin-tDNA	Streptavidin–biotin-cDNA	0.37 ng mL^{-1}	Dalirirad et al. (2020)
HPV16-DNA	CuO–DNA	Streptavidin–biotin-tDNA	Streptavidin–biotin-cDNA	1.0 nM	Yang et al. (2019)
Vaspin	UCNP–aptamer2	Streptavidin–biotin-aptamer1	Streptavidin–biotin-aptamer	39 pg mL^{-1}	Ali et al. (2020)
Thrombin	AuNP–Apt	Streptavidin–tDNA and thrombin	Streptavidin–cDNA	0.85 nM	Gao et al. (2019)
NPR or cTnI	AuNP–PRA70A	Anti-NPR or anti-cTnI Ab	Streptavidin–biotin-cDNA	0.26 pg mL^{-1} for NPR and 0.23 pg mL^{-1} for cTnI	Kang et al. (2019)
OPN	AuNP–streptavidin	Ab	ssDNA	0.1 ng mL^{-1}	Mukama et al. (2020)
β-conglutin	Fe_3O_4@AuNP–aptamer2-HRP	Aptamer1	NA	8 fM	Wu et al. (2018c)
PDGF-BB	$AuNP_B$–Ab_3/Cy3–$AuNP_A$–Ab_1	Streptavidin	Ab_2	1 ng mL^{-1}	Cheng et al. (2020)
RGNNV-CP	AuNP–DNA	tDNA	cDNA	5 ng mL^{-1}	Liu et al. (2020)
Erythromycin	AuNP–streptavidin	Ab	Biotin	3 pM	Du et al. (2021)
miRNA-21, -155, and −210	AuNP–SH-21, -155, and −210	Streptavidin–biotin-T-21, -155, and −210	Streptavidin–biotin-cDNA	0.073, 0.061, and 0.085 nM	Zheng et al. (2018)
PDGF-BB and thrombin	AuNP–aptamers of PDGF-BB and thrombin	Streptavidin–biotin-aptamers of PDGF-BB and thrombin	Streptavidin–biotin-cDNA	1 nM for PDGF-BB and 2 nM for thrombin	Liu et al. (2019)

NA: not available.

weaker than the TBL and much stronger than the TL. At moderate levels of thrombin, more AuNP–Apt/thrombin complexes were captured on the TL, and so generated a strong red band. The unreacted AuNP–Apt detection probes were then captured on the TBL, forming a weak red band. An even smaller number of AuNP–Apt detection probes were captured on the CL, formed a weaker red band. At ultra-high levels of thrombin, there are likely to be a large number of unreacted thrombin molecules in the mixture after the combination of thrombin and AuNP–Apt detection probes. Since the thrombin molecule is much smaller than the AuNP–Apt/thrombin complexes, thrombin, with the faster migration rate, would be captured by the tDNA on the TL first, which would inhibit the generation of sandwich complexes and result in a weak red band. Accordingly, fewer AuNP–Apt detection probes were captured by the thrombin on the TBL, leading to a weak red band. However, a large number of AuNP–Apt/thrombin complexes were captured by the cDNA, and a strong red band was generated on the CL. The linear range for thrombin was 1 nM–100 μM, with an LOD of 0.85 nM. The three-line sandwich format of aptamer-based LFA was capable of eliminating the influence of the hook effect, widening the detection range.

2.2. Sandwich LFA with a combination of aptamers and antibodies

Apart from the application of a pair of aptamers, the combination of aptamers and antibodies is utilized in the sandwich format of aptamer-based LFAs. Kang et al. reported a sandwich format LFA using both aptamer and antibody (Ab) for the detection of nucleoprotein (NPR) and cardiac troponin I (cTnI) in 10 min (Kang et al., 2019). In this assay, an ssDNA binding protein (PRA70A) was conjugated to the surface of AuNPs to form the detection probes (AuNP–PRA70A). Anti-NPR or anti-cTnI Ab was immobilized on the TL as the capture probe, and streptavidin-biotinylated cDNA against the NPR or cTnI specific aptamer was immobilized on the CL as the control probe. On adding a pre-incubated mixture of the target analyte and its aptamer to the sample pad, the Ab on the TL captured the target analyte. Afterwards, AuNP–PRA70A detection probes were applied to the sample pad to combine with the sandwich complex (AuNP–PRA70A-aptamer/target/Ab), making the color of the AuNPs detectable on the TL. The control probes on the CL captured the excess AuNP–PRA70A detection probes, resulting in a second red band. The LODs were 0.26 and 0.23 pg mL^{-1} for NPR and cTnI, respectively.

Using the same principle described above, Mukama et al. explored a sandwich format LFA to detect human osteopontin (OPN) in 5 min, as shown in Fig. 1(e) (Mukama et al., 2020). Streptavidin-modified AuNPs (AuNP–streptavidin) were dispersed on the conjugate pad as the detection probes, Ab for OPN and ssDNA complementary to the aptamer were immobilized on the TL and CL as the capture and control probes, respectively. When the mixture of OPN and biotinylated aptamer was applied to the sample pad, biotin-aptamer/OPN was initially bound to AuNP–streptavidin and then captured by Ab on the TL, generating a AuNP–streptavidin–biotin-aptamer/OPN/Ab sandwich with a red band. The excess AuNP–streptavidin was captured by ssDNA on the CL, forming a second red band. The linear range and LOD for OPN were 10–500 and 0.1 ng mL^{-1}, respectively.

2.3. Sandwich LFA with signal amplification strategies

To enhance the sensitivity, different signal amplification strategies have been exploited in the sandwich format of aptamer-based LFAs. Wu et al. prepared a sandwich LFA combined with enzyme amplification and magnetic enrichment for the detection of β-conglutin in 20 min (Wu et al., 2018c). In this assay, magnetic Fe_3O_4@AuNPs with a core-shell structure were prepared in order to conjugate with secondary aptamers to form the detection probes. Primary aptamers were immobilized on the TL as the capture probes. For enhanced sensitivity, horseradish peroxidase (HRP) was modified on the surface of Fe_3O_4@AuNPs *via* a streptavidin–biotin affinity reaction. With the addition of 3,3′,5,5′-tetramethylbenzidine (TMB), catalytic reaction between HRP and TMB

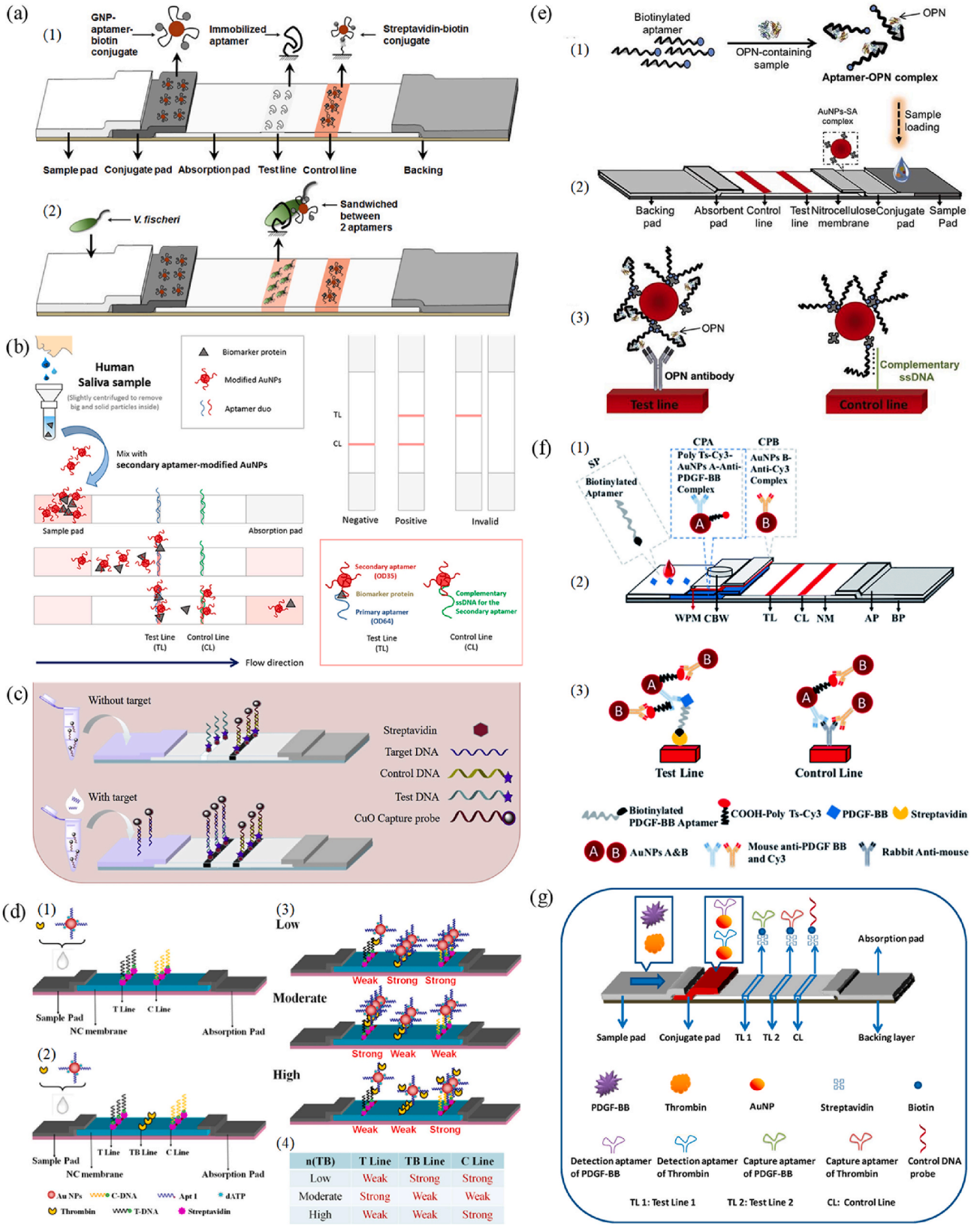

Fig. 1. (a) Sandwich LFA employing a pair of aptamers for the detection of *V. fischeri*, reproduced with permission from (Shin et al., 2018), copyright 2018 ACS; (b) sandwich LFA using ssDNA on the CL for the detection of ODAM, reproduced with permission from (Lee et al., 2019), copyright 2019 Elsevier; (c) sandwich LFA using CuO NPs as the label for the detection of HPV16-DNA, reproduced with permission from (Yang et al., 2019), copyright 2019 Elsevier; (d) three-line sandwich LFA for the detection of thrombin, reproduced with permission from (Gao et al., 2019), copyright 2019 Elsevier; (e) sandwich LFA using aptamers and antibodies to detect OPN, reproduced with permission from (Mukama et al., 2020), copyright 2020 Elsevier; (f) sandwich LFA using two different AuNPs for the detection of PDGF-BB, reproduced with permission from (Cheng et al., 2020), copyright 2020 RCS; (g) sandwich LFA for the multiplexed detection of PDGF-BB and thrombin, reproduced with permission from (Liu et al., 2019), copyright 2019 MDPI.

occurred, leading to an enhanced blue signal. To further improve the sensitivity, an external magnetic field was applied in order to reduce the flow speed and increase the reaction time. As a consequence of these modifications, the sensitivity was improved by the increase in the number of sandwich complexes formed on the TL. The linear range achieved using ImageJ software was 10 fM to 100 pM, with an LOD of 8 fM for β-conglutin.

Subsequently, Cheng et al. constructed a sandwich LFA using two different AuNPs for the detection of platelet-derived growth factor-BB (PDGF-BB) within 10 min, as shown in Fig. 1(f) (Cheng et al., 2020). Biotinylated aptamers were dispersed on the sample pad, and $AuNP_A$ modified with poly-Ts oligonucleotide (Ts-Cy3) and monoclonal antibody (Ab_1) against PDGF-BB (Cy3–$AuNP_A$–Ab_1) were dispersed on the first conjugate pad. Streptavidin and rabbit anti-mouse polyclonal antibody (Ab_2) were immobilized on the TL and CL, respectively. When PDGF-BB was applied to the sample pad, it was initially bound to the aptamer and then to the Cy3–$AuNP_A$–Ab_1, which was captured by the streptavidin on the TL, forming a Cy3–$AuNP_A$–Ab_1/PDGF-BB/aptamer-biotin–streptavidin sandwich with a visual red band. For enhanced sensitivity, $AuNP_B$ conjugated with another monoclonal antibody (Ab_3) for Cy3 ($AuNP_B$–Ab_3) was dispersed on the second conjugate pad. Consequently, $AuNP_B$–Ab_3/Cy3–$AuNP_A$–Ab_1/PDGF-BB/aptamer-biotin–streptavidin complexes were formed on the TL. The Ab_2 on the CL could capture excess Cy3–$AuNP_A$–Ab_1 or $AuNP_B$–Ab_3, thus forming a second red band. The linear range and LOD obtained with the naked eye were 3–300 and 1 ng mL^{-1}, respectively.

Recently, Liu et al. proposed a sandwich LFA employing magnetic enrichment and isothermal strand displacement amplification (SDA) for the detection of coat protein of red-spotted grouper nervous necrosis virus (RGNNV-CP) in 5 min (Liu et al., 2020). AuNP–DNA was dispensed on the conjugate pad, tDNA and cDNA were immobilized on the TL and CL, respectively. Two aptamers (A-apt and C-apt) were initially incubated with RGNNV-CP, then interacted with streptavidin modified magnetic beads (MBs) to form A-apt/RGNNV-CP/C-apt-biotin–streptavidin MBs complex. After magnetic separation, the complex was transferred to conduct the SDA reaction for amplification, where the A-apt of the complex was utilized as the template. Finally, the SDA products (amplified ssDNA) were loaded onto the sample pad, they initially interacted with AuNP–DNA and then were captured by tDNA on the TL. The cDNA on the CL captured the excess AuNP–DNA. The LOD observed by the naked eye was 5 ng mL^{-1} for RGNNV-CP.

Lately, Du et al. constructed a sandwich LFA using magnetic enrichment and recombinase polymerase amplification (RPA) for the detection of erythromycin within 15 min (Du et al., 2021). In this assay, AuNP–streptavidin was dispensed on the conjugate pad, Ab against FAM and biotin were immobilized on the TL and CL, respectively. When erythromycin was present in the sample, aptamer Ery_06 was eluted from MBs. After magnetic separation, the eluted Ery_06/erythromycin sequences were applied as templates for amplification by RPA with biotin and FAM modified forward and reverse primers, respectively. Once the RPA products (amplified dsDNA) were loaded on the sample pad, they initially interacted with AuNP–streptavidin via streptavidin–biotin reaction, then were captured by the Ab on the TL, forming AuNP–streptavidin/dsDNA/Ab sandwich with a red band. The biotin on the CL captured excess AuNP–streptavidin, generating a second red band. The LOD with the naked eye was 3 pM for erythromycin.

2.4. Sandwich LFA for multiplexed detection

Multiplexed detection, i.e., simultaneous detection of multiple target analytes in a single assay, has emerged in the sandwich format of aptamer-based LFAs. Zheng et al. described a sandwich LFA for the multiplexed detection of microRNA (miRNA)-21, −155, and −210 (Zheng et al., 2018). In this assay, three thiolated ssDNA probes (SH-21, SH-155, and SH-21 probes) were conjugated with AuNPs as the detection probes. Four streptavidin-biotin-ssDNA probes (T-21, T-155, T-210, and C probes) were then immobilized on the TL_1, TL_2, TL_3, and CL, respectively. The LODs were 0.073, 0.061, and 0.085 nM for miRNA-21, miRNA-155, and miRNA-210, respectively.

Subsequently, Liu et al. introduced a sandwich LFA for the multiplexed detection of PDGF-BB and thrombin in 10 min (Liu et al., 2019). As shown in Fig. 1(g), thiolated aptamers of PDGF-BB and thrombin were adopted to conjugate with AuNPs as the two detection probes. Streptavidin-biotinylated aptamers of PDGF-BB and thrombin were immobilized on the TL_1 and TL_2 as the two capture probes. Streptavidin-biotinylated DNA with a sequence complementary to that of the two detection probes was immobilized on the CL as the control probe. The LODs detected using a reader were 1 nM for PDGF-BB and 2 nM for thrombin.

3. Competitive format for aptamer-based LFAs

The competitive format of the aptamer-based LFA is generally utilized for the detection of analytes with only one epitope. The intuitive approach of competition uses the fact that the target in the sample competes with its complementary DNA on the TL to combine with the labeled aptamer. An alternative approach uses the fact that the target in the sample competes with its hapten on the TL to combine with the labeled aptamer. To improve the sensitivity, different signal amplification strategies have been utilized in the competitive format of aptamer-based LFAs. Nowadays, multiplexed detection in the competitive format of aptamer-based LFAs is of great interest to researchers. A summary of competitive format for aptamer-based LFAs is listed in Table 3.

3.1. Competition between the target and its complementary DNA

Based on the competition between the target in a sample and its complementary DNA on the TL for binding to labeled aptamer, Wu et al. designed a competitive LFA for the detection of zearalenone (ZEN) in corn samples in 5 min (Wu et al., 2018a). As shown in Fig. 2(a), AuNP–Apt was dispersed on the conjugate pad as the detection probe, while streptavidin-biotinylated DNA_1 and DNA_2 complementary to different fragments of the aptamer were immobilized on the TL and CL as the capture and control probes, respectively. In the presence of ZEN in the sample, ZEN initially combined with the AuNP–Apt detection probes, resulting in a decrease in available AuNP–Apt captured by the streptavidin-biotinylated DNA_1 capture probes, forming a weaker red band. Therefore, the less ZEN in the sample, the stronger the red band observed on the TL. Regardless of whether ZEN was in the sample or not, the AuNP–Apt detection probes were captured by the streptavidin-biotinylated DNA_2 control probes on the CL, evidencing that the LFA was working correctly. The linear range was 5–200 ng mL^{-1}, with an LOD of 20 ng mL^{-1}. Using the same principle described above, Gong et al. presented a competitive LFA for the detection of *N*-glycolylneuraminic acid (Neu5Gc) within 15 min (Gong et al., 2018). AuNP–Apt detection probes were dispersed on the conjugate pad, while capture and control probes complementary to different fragments of the aptamer were immobilized on the TL and CL, respectively. The semi-quantitative LOD obtained with the naked eye was 20 ng mL^{-1}, while the quantitative LOD detected using a reader was 5.38 ng mL^{-1}. Subsequently, Yu et al. introduced a competitive format for the detection of A549 exosomes (Yu et al., 2020). The CD63 aptamer was modified onto the surface of AuNPs to form the detection probes AuNP–CD63, and a streptavidin–biotin-CD63 aptamer complementary strand was immobilized on the TL. The visual LOD was 6.4×10^9 particles/mL.

Apart from the application of the DNA complementary to the aptamer as the control probe on the CL, antibodies are also applied as control probes in the competitive format of aptamer-based LFAs. Sun et al. described a competitive LFA using antibodies as the control probes to detect mercury(II) ions (Hg^{2+}) within 10 min, as shown in Fig. 2(b) (Sun et al., 2019). AuNP–DNA_1 was prepared for dispersion on the

Table 3
A summary of competitive format for aptamer-based LFAs.

Target analyte	Detection probe	TL	CL	LOD	Reference
ZEN	AuNP–Apt	Streptavidin–biotin-DNA_1	Streptavidin–biotin-DNA_2	20 ng mL^{-1}	Wu et al. (2018a)
Neu5Gc	AuNP–Apt	Streptavidin–biotin-tDNA	Streptavidin–biotin-cDNA	20 ng mL^{-1} with naked eye and 5.38 ng mL^{-1} with a reader	Gong et al. (2018)
A549 exosomes	AuNP–CD63	Streptavidin–biotin-tDNA	NA	6.4×10^9 particles/mL	Yu et al. (2020)
Hg^{2+}	AuNP–DNA_1-digoxin	Streptavidin–biotin-DNA_2	Digoxin Ab	2 ppb	Sun et al. (2019)
OTA	Cy5–Apt	Streptavidin–biotin-cDNA	Streptavidin–biotin-probe 2	0.4 ng mL^{-1}	Zhang et al. (2018b)
AFB_1	Cy5–Apt	Streptavidin–biotin-cDNA	Streptavidin–biotin-poly T	0.16 ng mL^{-1}	Zhao et al. (2020)
OTA	UCNP–Apt	Streptavidin–$cDNA_1$	Streptavidin–$cDNA_2$	1.86 ng mL^{-1}	Wu et al. (2018b)
AFB_1	Cy5–Apt	AFB_1-hapten	Streptavidin–biotin-probe	0.1 ng mL^{-1}	Zhu et al. (2018)
Kanamycin	AgNP–DNA_1/AuNP–Apt	Streptavidin–biotin-DNA_2	Streptavidin	0.0778 nM	Liu et al. (2018)
CA125	AuNP–CA125	Aptamer	NA	5.21 U/mL	Tripathi et al. (2020)
Hg^{2+}, OTA, and SE	UCNP–Apt_1, Apt_2, and Apt_3	DNA_1, DNA_2, and DNA_3	DNA	5 ppb for Hg^{2+}, 3 ng mL^{-1} for OTA, and 85 CFU mL^{-1} for SE	Jin et al. (2018)

NA: not available.

conjugate pad as the detection probe, while streptavidin-biotinylated DNA_2 and digoxin antibodies were immobilized on the TL and CL as the capture and control probes, respectively. Hg^{2+} in the sample competed with the DNA_2 capture probes to bind the AuNP–DNA_1 detection probes. Since DNA_1 was modified with digoxin, digoxin antibodies on the CL captured excess AuNP–DNA_1, thus forming a red band. The LOD obtained with the naked eye or bionic e-Eye imaging was 2 parts per billion (ppb).

Recently, fluorescent nanoparticles have been utilized in the competitive format of aptamer-based LFAs. Zhang et al. proposed a competitive LFA using fluorescent Cy5 as the label for the detection of ochratoxin A (OTA) in 20 min (Zhang et al., 2018b). As shown in Fig. 2 (c), Cy5–Apt was dispersed on the conjugate pad as the detection probe. Streptavidin-biotinylated cDNA and probe 2 complementary to different fragments of OTA aptamer were immobilized on the TL and CL as the capture and control probes, respectively. In the presence of OTA, Cy5–Apt/OTA complexes were generated and fewer Cy5–Apt molecules were captured on the TL, leading to a decrease in fluorescent signals. In the absence of OTA, Cy5–Apt was captured by Streptavidin-biotinylated cDNA on the TL, generating a strong fluorescence signal. The quantitative linear range and LOD for OTA using a reader were 1–1000 and 0.4 ng mL^{-1}, respectively. Subsequently, Wu et al. reported a competitive LFA using UCNPs ($NaYF_4$:Yb,Er) as the label for detecting OTA in 15 min (Wu et al., 2018b). UCNP–Apt was dispersed on the conjugate pad as the detection probe. $cDNA_1$ and $cDNA_2$ complementary to different fragments of OTA aptamer were immobilized on the TL and CL as the capture and control probes, respectively. The linear range was 5–100 ng mL^{-1}, with an LOD of 1.86 ng mL^{-1}.

3.2. Competition between the target and its hapten

The competition between the target in the sample and the target–hapten on the TL for binding to the labeled aptamer is an alternative approach applied in the competitive format of aptamer-based LFAs. Zhu et al. developed a dual competitive LFA using fluorescent Cy5 for the detection of aflatoxin B_1 (AFB_1) in food samples within 20 min, as shown in Fig. 2(d) (Zhu et al., 2018). This assay was based on the competition for Cy5–Apt between the target AFB_1 in the sample and the AFB_1-hapten on the TL. Additionally, the streptavidin-biotinylated complementary probe competed with the target AFB_1 for binding to Cy5–Apt on the CL. In the presence of AFB_1 in the sample, abundant Cy5–Apt/AFB_1 complexes were generated, and limited Cy5–Apt was captured by the AFB_1-BSA immobilized on the TL, resulting in a decrease in the fluorescent signal. Due to stronger affinity between the aptamer and its complementary strand, Cy5–Apt was dissociated from the Cy5–Apt/AFB_1 complexes and then captured on the CL. Therefore, the fluorescent signal on the TL was negatively correlated with AFB_1 concentration, whereas the fluorescent signal on the CL was positively correlated with AFB_1 concentration. The linear range for AFB_1 was 0.1–1000 ng mL^{-1}, with an LOD of 0.1 ng mL^{-1}.

3.3. Competitive LFA with signal amplification strategies

To improve the sensitivity, signal amplification strategies have also been applied to the competitive format of aptamer-based LFAs. Liu et al. established a competitive LFA using silver nanoparticles (AgNPs) as the signal amplification strategy for the detection of kanamycin in 10 min (Liu et al., 2018). As shown in Fig. 2(e), AuNP–Apt was dispersed on the conjugate pad as the detection probe. Additionally, streptavidin–biotin-DNA_2 and streptavidin were immobilized on the TL and CL as the capture and control probes, respectively. For enhanced sensitivity, oligonucleotide DNA_1 complementary to the aptamer at the 5′-terminal and the DNA_2 at its 3′-terminal were applied in order to modify AgNPs (AgNP–DNA_1) as the signal amplification element, which was also dispersed on the conjugate pad. In the absence of kanamycin, AgNP–DNA_1/AuNP–Apt complexes were initially formed and further captured by DNA_2 on the TL, forming a clear red band, while, in the presence of kanamycin, the latter was bound specifically to the AuNP–Apt detection probes, leading to fewer AgNP–DNA_1/AuNP–Apt complexes formed and then captured by DNA_2 on the TL, thus generating a lighter or faded red band. Regardless of whether kanamycin was present in the sample or not, excess AuNP–Apt was captured on the CL through the biotin–streptavidin interaction. The qualitative LOD for kanamycin obtained with the naked eye was 35 nM, while the quantitative linear range and LOD detected by a reader were 1–30 and 0.0778 nM, respectively.

More recently, Tripathi et al. prepared a competitive LFA using nanozymes as the signal amplification strategy for the detection of CA125 in human serum within 20 min (Tripathi et al., 2020). AuNP–CA125 was dispersed on the conjugate pad as the detection probe, while CA125 aptamer was immobilized on the TL as the capture probe. For improved sensitivity, AuNPs captured on the TL were applied as a peroxidase mimetic to catalyze the oxidation of the DAB/H_2O_2 substrate. The linear range for CA125 was 7.5–200 U/mL, with an LOD of 5.21 U/mL.

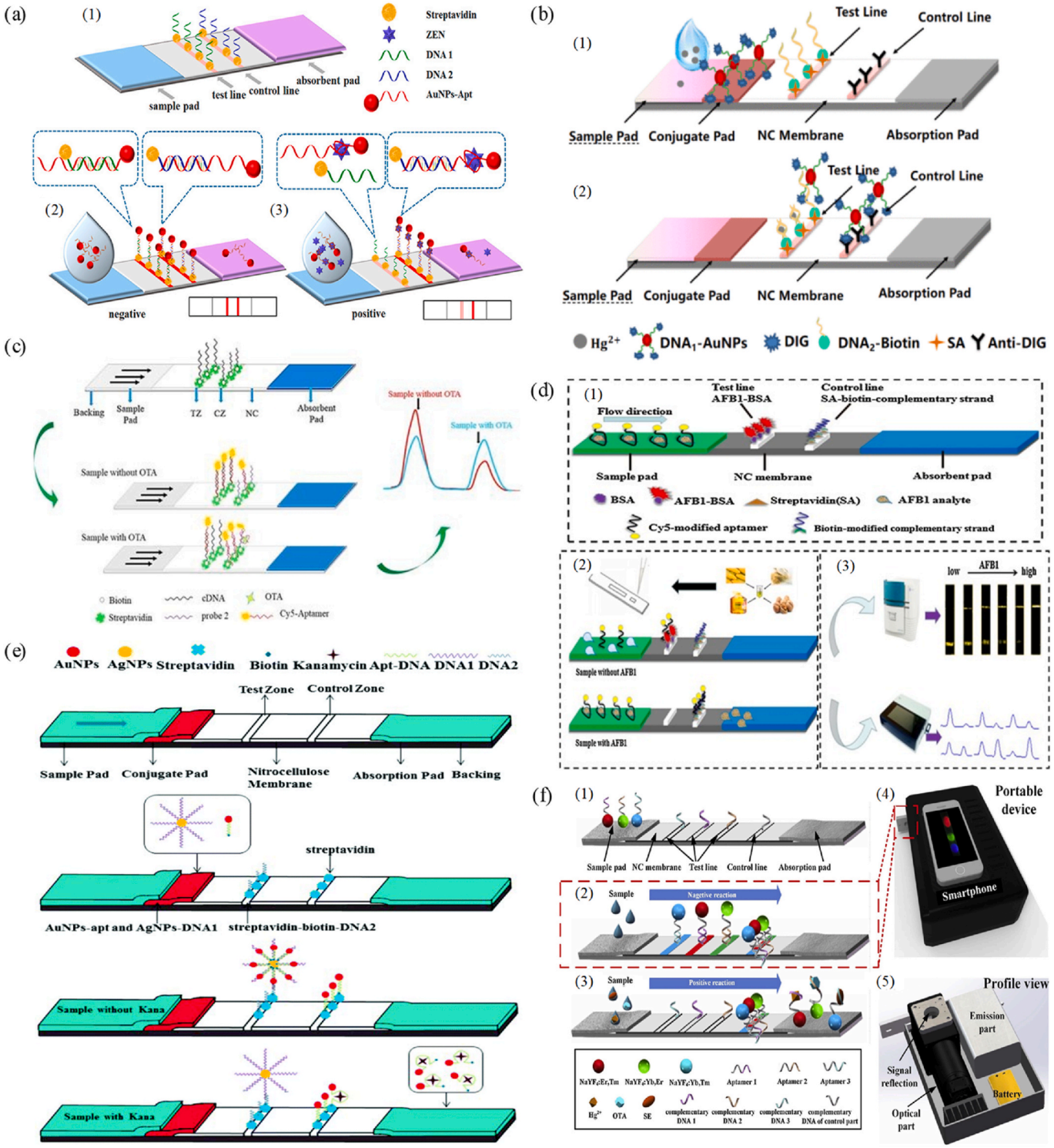

Fig. 2. (a) Competitive LFA for the detection of ZEN, reproduced with permission from (Wu et al., 2018a), copyright 2018 ACS; (b) competitive LFA using antibodies as the control probes to detect Hg^{2+}, reproduced with permission from (Sun et al., 2019), copyright 2019 IEEE; (c) competitive LFA using fluorescent Cy5 as the label for the detection of OTA, reproduced with permission from (Zhang et al., 2018b), copyright 2018 MDPI; (d) dual competitive LFA using fluorescent Cy5 for the detection of AFB_1, reproduced with permission from (Zhu et al., 2018), copyright 2018 Elsevier; (e) competitive LFA using AgNPs as signal amplification strategy for the detection of kanamycin, reproduced with permission from (Liu et al., 2018), copyright 2018 RSC; (f) competitive LFA for the multiplexed detection of Hg^{2+}, OTA, and SE, reproduced with permission from (Jin et al., 2018), copyright 2018 Elsevier.

3.4. Competitive LFA for multiplexed detection

Multiplexed detection has been applied to the competitive format of aptamer-based LFAs currently produced. Jin et al. constructed a competitive LFA for the multiplexed detection of Hg^{2+}, OTA, and *Salmonella* (SE) in 30 min, as shown in Fig. 2(f) (Jin et al., 2018). Multicolored UCNPs were modified with three aptamers (red $NaYF_4$:Er, Tm@$NaYF_4$–Apt_1 for Hg^{2+}, green $NaYF_4$:Yb,Er–Apt_2 for OTA, and blue $NaYF_4$:Yb,Tm–Apt_3 for SE) as the detection probes. DNA_1 complementary to Apt_1, DNA_2 complementary to Apt_2, DNA_3 complementary to

Apt_3, and DNA complementary to all aptamers were immobilized on three TLs and one CL as three capture probes and one control probe, respectively. A smartphone-based device was used to read the color intensities. The linear ranges were 10–10^4 ppb for Hg^{2+}, 0.01–50 μg mL^{-1} for OTA, and 150–2000 CFU mL^{-1} for SE, while the LODs were 5 ppb for Hg^{2+}, 3 ng mL^{-1} for OTA, and 85 CFU mL^{-1} for SE.

4. Adsorption–desorption format for aptamer-based LFAs

Due to the distinctive ability of aptamers to undergo conformational changes, the adsorption–desorption format has been exploited in aptamer-based LFAs. This format depends on the adsorption of aptamer onto the surface of labels and the subsequent desorption from the labeled aptamer as the aptamer combines preferentially with the target. To accomplish the adsorption–desorption format, labeled aptamer or duplex aptamers have been explored in aptamer-based LFAs. For enhanced sensitivity, signal amplification strategies have also been applied. A summary of adsorption–desorption format for aptamer-based LFAs is listed in Table 4.

4.1. Adsorption-desorption LFA with labeled aptamer

The adsorption–desorption format with labeled aptamer has been investigated in aptamer-based LFAs currently being produced. Ranganathan et al. established an adsorption–desorption LFA for the detection of human epidermal growth factor receptor 2 (HER2), as shown in Fig. 3 (a) (Ranganathan et al., 2020). Biotinylated aptamers were adsorbed onto the surface of AuNPs to form AuNP–Apt detection probes. Streptavidin and poly(diallyldimethylammonium chloride) (PDDA) polymer were immobilized on the TL and CL as the capture and control probes, respectively. In the presence of HER2, the latter initially bound with the aptamers to release AuNPs, causing no red dot on the TL. Instead, free AuNPs were captured by the charged PDDA polymer and then aggregated on the CL. In the absence of HER2, AuNP–Apt was captured by streptavidin to form a red dot on the TL. The visual LODs for HER2 were 20 nM in water and 24 nM in human serum.

Similarly, Velu et al. constructed an adsorption–desorption LFA for the detection of OTA (Velu and DeRosa, 2018). Biotinylated A08min-aptamers were adsorbed onto the surface of AuNPs to form AuNP–Apt detection probes. Streptavidin and PDDA polymer were immobilized on the TL and CL as the capture and control probes, respectively. The LOD was 6.3 nM.

Recently, Dalirirad et al. presented an adsorption–desorption LFA for the detection of cortisol in sweat (Dalirirad and Steckl, 2019). Aptamers were adsorbed onto the surface of AuNPs to form AuNP–Apt detection probes, which were dispersed on the conjugate pad. Additionally, cysteamine was immobilized on the TL as the capture probe. In the presence of cortisol, the latter initially interacted with the AuNP–Apt, causing aptamers to be desorbed from the surface of the AuNPs. As a consequence, free AuNPs were captured by cysteamine and aggregated on the TL. The visual LOD obtained with a hand-held device was 1 ng mL^{-1}.

4.2. Adsorption-desorption LFA with labeled duplex aptamers

In recent years, the adsorption–desorption format with labeled duplex aptamers has also been explored in aptamer-based LFAs. Alnajrani et al. reported an adsorption–desorption LFA for the detection of progesterone (P4) (Alnajrani and Alsager, 2019). AuNPs functionalized with P4-aptamer and biotinylated complementary sequence were prepared in order to form an AuNP–Apt duplex as the detection probe. In the absence of P4, the AuNP–Apt duplex was captured by streptavidin on the TL *via* the streptavidin–biotin reaction, generating an intense red band. In the presence of P4, the biotinylated complementary sequence was released from the AuNP–Apt duplex due to the conformational change, causing the red band to disappear. The LOD was 4 nM, which was a 20-fold improvement.

Similarly, Dalirirad et al. developed an adsorption–desorption LFA for the detection of dopamine in urine (Dalirirad and Steckl, 2020). As shown in Fig. 3(b), dopamine duplex aptamer, prepared by hybridizing dopamine aptamer (DNA_2) and capture aptamer (DNA_3), was immobilized on the surface of AuNPs *via* a 20 T linker (DNA_1) to form an AuNP–Apt duplex, which was then dispersed on the conjugate pad as the detection probe. Streptavidin-biotinylated $cDNA_3$ complementary to DAN_3 and $cDNA_1$ complementary to $cDNA_1$ were immobilized on the TL and CL as the capture and control probes, respectively. In the presence of dopamine, DNA_2 was dissociated from the AuNP–Apt duplex to interact with dopamine, causing DNA_3 to be captured by $cDNA_3$ on the TL, while in the absence of dopamine, no free DNA_3 was available to hybridize with $cDNA_3$ on the TL. Regardless of whether dopamine was present in the sample or not, DNA_1 in the AuNP–Apt duplex was captured by $cDNA_1$ on the CL, indicating that the LFA was working correctly. The LOD detected by the ImageJ software was 10 ng mL^{-1}, and the visual LOD was 50 ng mL^{-1}.

4.3. Adsorption–desorption LFA with signal amplification strategies

To enhance the sensitivity, SDA has been investigated in the adsorption–desorption format of aptamer-based LFAs. Recently, Deng et al. proposed an adsorption–desorption fluorescent LFA using CdTe quantum dots (QDs) to detect HIV-DNA within 15 min (Deng et al., 2018). As shown in Fig. 3(c), streptavidin-biotinylated tDNA and cDNA were immobilized on the TL and CL as capture and control probes, respectively. Two kinds of hairpin DNAs (H1 and H2) were utilized in the LFA, where H1 had a trigger complementary to HIV-DNA and H2 was modified with CdTe as the detection probes. In the absence of HIV-DNA, H1 was incapable of binding to H2, while in the presence of HIV-DNA, it initially bound to the trigger of H1, forming a H1/HIV-DNA

Table 4
A summary of adsorption–desorption format for aptamer-based LFAs.

Target analyte	Detection probe	TL	CL	LOD	Reference
HER2	AuNP-Apt-biotin	Streptavidin	PDDA polymer	20 nM in water and 24 nM in human serum	Ranganathan et al. (2020)
OTA	AuNP-Apt-biotin	Streptavidin	PDDA polymer	6.3 nM	Velu and DeRosa (2018)
Cortisol	AuNP–Apt	Cysteamine	NA	1 ng mL^{-1}	Dalirirad and Steckl (2019)
P4	AuNP-Apt duplex	Streptavidin	NA	4 nM	Alnajrani and Alsager (2019)
dopamine	AuNP–Apt duplex	Streptavidin–biotin-$cDNA_3$	Streptavidin–biotin-$cDNA_1$	50 ng mL^{-1}	Dalirirad and Steckl (2020)
HIV-DNA	CdTe–H2/H1	Streptavidin–biotin-tDNA	Streptavidin–biotin-cDNA	0.76 pM	Deng et al. (2018)
L. monocytogenes	Aptamer-gated $mSiO_2$ with TMB	HRP	NA	53 cells/mL	Tasbasi et al. (2019)

NA: not available.

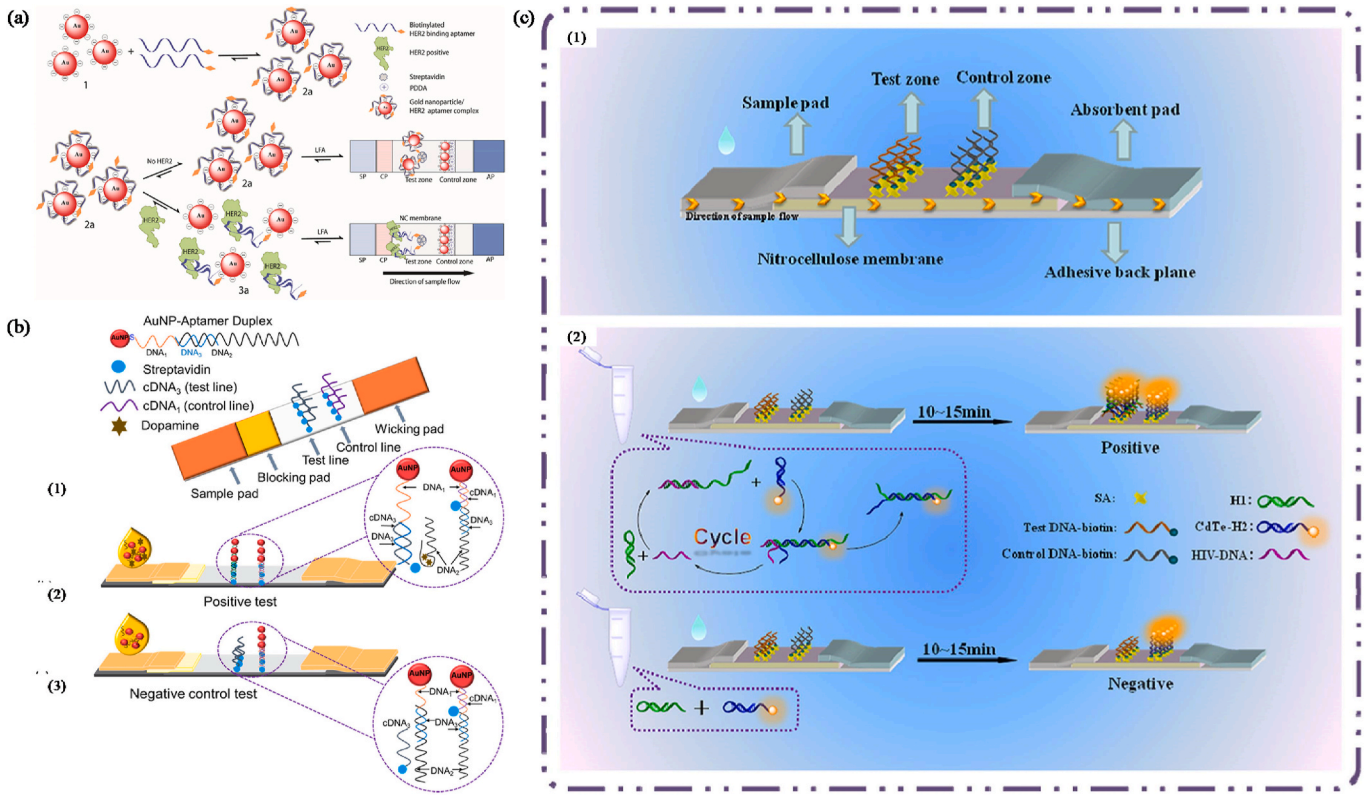

Fig. 3. (a) Adsorption–desorption LFA with labeled aptamer for the detection of HER2, reproduced with permission from (Ranganathan et al., 2020), copyright 2019 Elsevier; (b) adsorption–desorption LFA with labeled duplex aptamers for the detection dopamine, reproduced with permission from (Dalirirad and Steckl, 2020), copyright 2020 Elsevier; (c) adsorption–desorption fluorescent LFA using CdTe QDs to detect HIV-DNA, reproduced with permission from (Deng et al., 2018), copyright 2018 Elsevier.

structure. Since the unfolded part of H1 was complementary to H2, a CdTe–H2/H1/HIV-DNA complex was generated. Due to strand displacement, the HIV-DNA separated from the complex and participated in the next reaction cycle. Eventually, a small amount of HIV-DNA was converted into a very large number of CdTe–H2/H1 conjugates, which were captured by tDNA on the TL. As CdTe–H2/H1 instead of HIV-DNA was captured on the TL, the hook effect resulting from inappropriate ratios of labeled aptamers and targets could be effectively eliminated. The linear range obtained with a reader was 1 pM–10 nM, with an LOD of 0.76 pM.

Based on the conformational changes of aptamers that release entrapped reporter molecules, aptamer-gated silica nanoparticles have been exploited as a signal amplification approach in the adsorption–desorption format of aptamer-based LFAs. Tasbasi et al. developed an adsorption–desorption label-free LFA employing aptamer-gated mesoporous silica nanoparticles ($mSiO_2$) for the detection of *Listeria monocytogenes* (*L. monocytogenes*) within 5 min (Tasbasi et al., 2019). In this assay, aptamer-gated $mSiO_2$ loaded with TMB molecules were dispersed on the conjugate pad as the detection probes, while HRP was immobilized on the TL as the capture probe. In the presence of *L. monocytogenes*, the latter interacted with the aptamer-gated $mSiO_2$ to release TMB from the nanopores. Subsequently, an oxidation reaction between TMB and HRP occurred on the TL, forming a blue precipitate. The LOD for *L. monocytogenes* obtained with the ImageJ software was 53 cells/mL.

5. Conclusions

In recent years, aptamers have been thoroughly explored as biorecognition molecules in LFAs for the on-site detection of diverse target analytes, including proteins and even small molecules. Compared to antibodies counterparts, aptamers screened through an *in vitro* process can avoid the risk of killing the animal hosts, making it possible to screen aptamers against non-immunogenic molecules (Hassani et al., 2018). Although the selection process of aptamers may be expensive, once aptamers are successfully screened, the cost of synthesizing aptamers can be remarkably lower than that of antibodies (Hassani et al., 2017). Additionally, aptamers with higher reproducibility and chemical stability can avoid errors between different batches and refrigerated conditions for storing them (Hassani et al. 2020a, 2020b). Due to the inherent nature of nucleic acids, aptamers are also capable of recovering their conformation following denaturation, allowing them to flexibly adapt to different assay formats that are not available with antibodies (Salek Maghsoudi et al., 2020). Applications for the detection of target analytes with three formats of aptamer-based LFAs, i.e., sandwich, competitive, and adsorption–desorption, are shown in Fig. 4.

Although the outstanding advantages of aptamers, the practical applications of aptamer-based LFAs have not been commercialized yet. Therefore, it is essential to deal with several obstacles that hinder the commercialization of aptamer-based LFAs. Generally, the application of aptamers to LFAs is regarded as proof-of-concept for novel on-site biosensors, and only a few aptamers have been successfully applied in LFAs. To address this, researchers must focus on the analytes that are urgently needed by end-users in market. For example, coronavirus disease 2019 (COVID-19) caused by Severe Acute Respiratory Syndrome Corona Virus (SARS-CoV-2) has been an incomparable global public health emergency (Cui and Zhou, 2020; Orooji et al., 2020; Verma et al., 2020). As per the World Health Organization (WHO), more than 102 million confirmed cases with over 2 million deaths have been reported (https://covid19.who.int/). Therefore, the development of aptamer-based LFAs for newly emerged analytes such as SARS-CoV-2 may be a promising approach to facilitate commercialization. Recently, the Aptamer

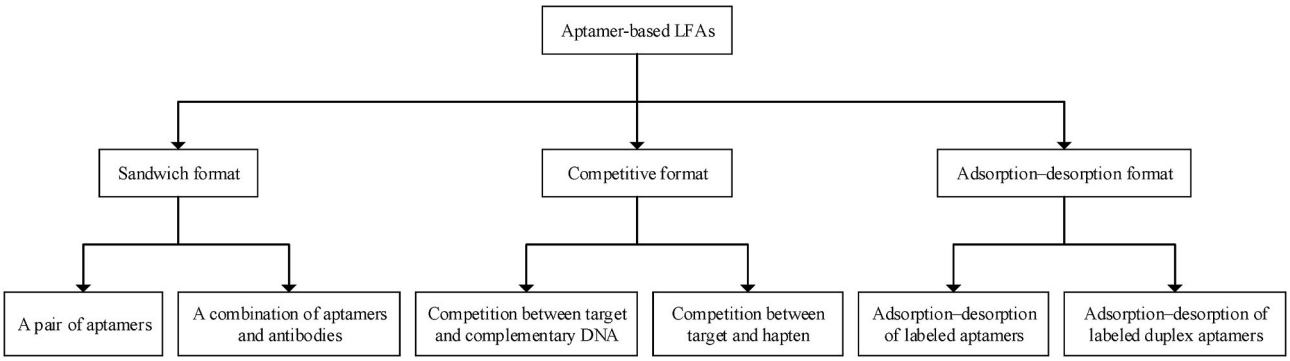

Fig. 4. Applications for the detection of target analytes with three formats of aptamer-based LFAs, i.e., sandwich, competitive, and adsorption–desorption.

Group Ltd. is trailing a sandwich aptamer-based LFA using dual aptamers of spike proteins (S1 and S2) for the rapid detection of SARS-CoV-2 S protein in saliva to support the COVID-19 pandemic (https://aptamergroup.com/lfd/).

The choice of NC membrane, the size of pores, and the applications of nanoparticles in aptamer-based LFAs have not been extensively explored. The NC membrane employed to immobilize capture and control molecules plays an essential role in the analytical performance of aptamer-based LFAs. The affinity reaction between streptavidin and biotin has been the most widely accepted method for immobilization of aptamers, where streptavidin initially immobilized on the NC membrane can react with biotinylated aptamer to form stable capture and control probes. Additionally, the pore size of NC membrane controls the flow rate of the loaded sample and further affects the sensitivity. A faster flow rate often results in a shorter reaction time and further causes a lower sensitivity. Whilst a slower flow rate leads to a longer reaction time, which usually increases the possibility of non-specific binding. Furthermore, AuNPs have been demonstrated as the most promising nanoparticles for the development of detection probes in aptamer-based LFAs. Through chemical or physical adsorption, aptamers can be modified on AuNPs to prepare detection probes. Due to the unique optical property of AuNPs, they can be easily recognized by naked eye for colorimetric detection. For improved sensitivity, optical nanoparticles such as CuO NPs and Fe_3O_4@AuNPs have been reported in aptamer-based LFAs. Different signal amplification strategies including enzyme amplification, magnetic enrichment, SDA, aptamer-gated silica nanoparticles, and RPA have been investigated to enhance the sensitivity. Fluorescent nanoparticles QDs and UCNPs have also been applied in aptamer-based LFAs to obtain quantitative analysis. Therefore, there is an urgent need to explore the choice of NC membrane, the size of pores, and the application of nanoparticles in aptamer-based LFAs for optimized analysis performance.

The test results obtained with the naked eye or through the use of ImageJ software often limit the widespread application of aptamer-based LFAs. To address this issue, smartphones, as the most widely used terminal devices, could also be applied for quantitative detection. Furthermore, aptamer-based LFAs combine with “big date” and fifth generation wireless communication technology will be a promising approach for real-time detection and remote analysis.

In summary, aptamers with the remarkable advantages of high affinity, low cost, and ease of modification can facilitate the application of LFAs for the on-site detection of target analytes. More attention is also required to reduce the complexity and costs of sandwich, competitive, and adsorption–desorption formats for aptamer-based LFAs. We strongly envision that advances in aptamer-based LFAs for on-site detection will continue to be made and be fully exploited in the future.

Declaration of competing interest

The authors declare that they have no known competing financial interests or personal relationships that could have appeared to influence the work reported in this paper.

Acknowledgements

The authors thank the financial support from the Shenzhen Science and Technology Program (KQTD20170809110344233), Shenzhen Bay Laboratory (SZBL2019062801005).

References

Ali, M., Sajid, M., Khalid, M.A.U., Kim, S.W., Lim, J.H., Huh, D., Choi, K.H., 2020. A fluorescent lateral flow biosensor for the quantitative detection of Vaspin using upconverting nanoparticles. Spectrochim. Acta Mol. Biomol. Spectrosc. 226.
Alnajrani, M.N., Alsager, O.A., 2019. Lateral flow aptasensor for progesterone: competitive target recognition and displacement of short complementary sequences. Anal. Biochem. 587.
Amraee, M., Oloomi, M., Yavari, A., Bouzari, S., 2017. DNA aptamer identification and characterization for E-coli O157 detection using cell based SELEX method. Anal. Biochem. 536, 36–44.
Bahadir, E.B., Sezginturk, M.K., 2016. Lateral flow assays: principles, designs and labels. Trac. Trends Anal. Chem. 82, 286–306.
Banerjee, R., Jaiswal, A., 2018. Recent advances in nanoparticle-based lateral flow immunoassay as a point-of-care diagnostic tool for infectious agents and diseases. Analyst 143 (9), 1970–1996.
Bruno, J.G., Carrillo, M.P., Richarte, A.M., Phillips, T., Andrews, C., Lee, J.S., 2012. Development, screening, and analysis of DNA aptamer libraries potentially useful for diagnosis and passive immunity of arboviruses. BMC Res. Notes 5, 633-633.
Chen, A., Yang, S., 2015. Replacing antibodies with aptamers in lateral flow immunoassay. Biosens. Bioelectron. 71, 230–242.
Chen, Y., Sun, J., Xianyu, Y., Yin, B., Niu, Y., Wang, S., Cao, F., Zhang, X., Wang, Y., Jiang, X., 2016. A dual-readout chemiluminescent-gold lateral flow test for multiplex and ultrasensitive detection of disease biomarkers in real samples. Nanoscale 8 (33), 15205–15212.
Cheng, N., Liu, Y., Mukama, O., Han, X., Huang, H., Li, S., Zhou, P., Lu, X., Li, Z., 2020. A signal-enhanced and sensitive lateral flow aptasensor for the rapid detection of PDGF-BB. RSC Adv. 10 (32), 18601–18607.
Chung, J., Kang, J.S., Jurng, J.S., Jung, J.H., Kim, B.C., 2015. Fast and continuous microorganism detection using aptamer-conjugated fluorescent nanoparticles on an optofluidic platform. Biosens. Bioelectron. 67, 303–308.
Cui, F., Zhou, H.S., 2020. Diagnostic methods and potential portable biosensors for coronavirus disease 2019. Biosens. Bioelectron. 165, 112349.
Dalirirad, S., Han, D., Steckl, A.J., 2020. Aptamer-based lateral flow biosensor for rapid detection of salivary cortisol. ACS Omega 5 (51), 32890–32898.
Dalirirad, S., Steckl, A.J., 2019. Aptamer-based lateral flow assay for point of care cortisol detection in sweat. Sensor. Actuator. B Chem. 283, 79–86.
Dalirirad, S., Steckl, A.J., 2020. Lateral flow assay using aptamer-based sensing for on-site detection of dopamine in urine. Anal. Biochem. 596.
Deng, X., Wang, C., Gao, Y., Li, J., Wen, W., Zhang, X., Wang, S., 2018. Applying strand displacement amplification to quantum dots-based fluorescent lateral flow assay strips for HIV-DNA detection. Biosens. Bioelectron. 105, 211–217.
Dhiman, A., Kaira, P., Bansal, V., Bruno, J.G., Sharma, T.K., 2017. Aptamer-based point-of-care diagnostic platforms. Sensor. Actuator. B Chem. 246, 535–553.
Diaz-Amaya, S., Lin, L.-K., Deering, A.J., Stanciu, L.A., 2019. Aptamer-based SERS biosensor for whole cell analytical detection of E. coli O157:H7. Anal. Chim. Acta 1081, 146–156.
Du, Y., Liu, D., Wang, M., Guo, F., Lin, J.S., 2021. Preparation of DNA aptamer and development of lateral flow aptasensor combining recombinase polymerase amplification for detection of erythromycin. Biosens. Bioelectron. 113157.
Fang, Z., Wu, W., Lu, X., Zeng, L., 2014. Lateral flow biosensor for DNA extraction-free detection of salmonella based on aptamer mediated strand displacement. amplification. Biosens. Bioelectron. 56, 192–197.

Farka, Z., Jurik, T., Kovar, D., Trnkova, L., Skladal, P., 2017. Nanoparticle-based immunochemical biosensors and assays: recent advances and challenges. Chem. Rev. 117 (15), 9973–10042.
Gao, Y., Zhu, Z., Xi, X., Cao, T., Wen, W., Zhang, X., Wang, S., 2019. An aptamer-based hook-effect-recognizable three-line lateral flow biosensor for rapid detection of thrombin. Biosens. Bioelectron. 133, 177–182.
Gong, S., Ren, H., Lin, C., Hu, P., Tian, R., Liu, Z., Li, Y., Zhou, Y., Yang, Y., Lu, S., 2018. Immunochromatographic strip biosensor for the rapid detection of N-glycolylneuraminic acid based on aptamer-conjugated nanoparticle. Anal. Biochem. 561, 52–58.
Gong, X., Cai, J., Zhang, B., Zhao, Q., Piao, J., Peng, W., Gao, W., Zhou, D., Zhao, M., Chang, J., 2017. A review of fluorescent signal-based lateral flow immunochromatographic strips. J. Mater. Chem. B 5 (26), 5079–5091.
Gopinath, S.C.B., Lakshmipriya, T., Chen, Y., Phang, W.-M., Hashim, U., 2016. Aptamer-based 'point-of-care testing. Biotechnol. Adv. 34 (3), 198–208.
Hassani, S., Akmal, M.R., Salek-Maghsoudi, A., Rahmani, S., Ganjali, M.R., Norouzi, P., Abdollahi, M., 2018. Novel label-free electrochemical aptasensor for determination of Diazinon using gold nanoparticles-modified screen-printed gold electrode. Biosens. Bioelectron. 120, 122–128.
Hassani, S., Maghsoudi, A.S., Akmal, M.R., Rahmani, S., Sarihi, P., Ganjali, M.R., Norouzi, P., Abdollahi, M., 2020a. A sensitive aptamer-based biosensor for electrochemical quantification of PSA as a specific diagnostic marker of prostate cancer. J. Pharm. Pharmaceut. Sci. 23, 243–258.
Hassani, S., Momtaz, S., Vakhshiteh, F., Maghsoudi, A.S., Ganjali, M.R., Norouzi, P., Abdollahi, M., 2017. Biosensors and their applications in detection of organophosphorus pesticides in the environment. Arch. Toxicol. 91 (1), 109–130.
Hassani, S., Rezaei Akmal, M., Salek Maghsoudi, A., Rahmani, S., Vakhshiteh, F., Norouzi, P., Ganjali, M.R., Abdollahi, M., 2020b. High-performance voltammetric aptasensing platform for ultrasensitive detection of bisphenol A as an environmental pollutant. Frontiers in Bioengineering and Biotechnology 8.
Huang, L., Tian, S., Zhao, W., Liu, K., Ma, X., Guo, J., 2020. Multiplexed detection of biomarkers in lateral-flow immunoassays. Analyst 145 (8), 2828–2840.
Huang, X., Aguilar, Z.P., Xu, H., Lai, W., Xiong, Y., 2016. Membrane-based lateral flow immunochromatographic strip with nanoparticles as reporters for detection: a review. Biosens. Bioelectron. 75, 166–180.
Huang, Y., Chen, X., Duan, N., Wu, S., Wang, Z., Wei, X., Wang, Y., 2015. Selection and characterization of DNA aptamers against Staphylococcus aureus enterotoxin C1. Food Chem. 166, 623–629.
Hyeon, J.-Y., Chon, J.-W., Choi, I.-S., Park, C., Kim, D.-E., Seo, K.-H., 2012. Development of RNA aptamers for detection of Salmonella Enteritidis. J. Microbiol. Methods 89 (1), 79–82.
Jauset-Rubio, M., El-Shahawi, M.S., Bashammakh, A.S., Alyoubi, A.O., O'Sullivan, C.K., 2017. Advances in aptamers-based lateral flow assays. Trac. Trends Anal. Chem. 97, 385–398.
Jin, B., Yang, Y., He, R., Park, Y.I., Lee, A., Bai, D., Li, F., Lu, T.J., Xu, F., Lin, M., 2018. Lateral flow aptamer assay integrated smartphone-based portable device for simultaneous detection of multiple targets using upconversion nanoparticles. Sensor. Actuator. B Chem. 276, 48–56.
Kang, J., Yeom, G., Jang, H., Oh, J., Park, C.-J., Kim, M.-G., 2019. Development of replication protein A-conjugated gold nanoparticles for highly sensitive detection of disease biomarkers. Anal. Chem. 91 (15), 10001–10007.
Kim, H., Chung, D.-R., Kang, M., 2019a. A new point-of-care test for the diagnosis of infectious diseases based on multiplex lateral flow immunoassays. Analyst 144 (8), 2460–2466.
Kim, S.H., Lee, J., Lee, B.H., Song, C.-S., Gu, M.B., 2019b. Specific detection of avian influenza H5N2 whole virus particles on lateral flow strips using a pair of sandwich-type aptamers. Biosens. Bioelectron. 134, 123–129.
Kim, Y.S., Raston, N.H.A., Gu, M.B., 2016. Aptamer-based nanobiosensors. Biosens. Bioelectron. 76, 2–19.
Kuhn, P., Fuehner, V., Unkauf, T., Moreira, G.M.S.G., Frenzel, A., Miethe, S., Hust, M., 2016. Recombinant antibodies for diagnostics and therapy against pathogens and toxins generated by phage display. Proteonomics Clin. Appl. 10 (9–10), 922–948.
Lee, B.H., Kim, S.H., Ko, Y., Park, J.C., Ji, S., Gu, M.B., 2019. The sensitive detection of ODAM by using sandwich-type biosensors with a cognate pair of aptamers for the early diagnosis of periodontal disease. Biosens. Bioelectron. 126, 122–128.
Li, J., Jing, L., Song, Y., Zhang, J., Chen, Q., Wang, B., Xia, X., Han, Q., 2018. Rapid detection of rongalite via a sandwich lateral flow strip assay using a pair of aptamers. Nanoscale Research Letters 13.
Liu, G., Gurung, A.S., Qiu, W., 2019. Lateral flow aptasensor for simultaneous detection of platelet-derived growth factor-BB (PDGF-BB) and thrombin. Molecules 24 (4).
Liu, G., Mao, X., Phillips, J.A., Xu, H., Tan, W., Zeng, L., 2009. Aptamer-Nanoparticle strip biosensor for sensitive detection of cancer cells. Anal. Chem. 81 (24), 10013–10018.
Liu, J., Qin, Q., Zhang, X., Li, C., Yu, Y., Huang, X., Mukama, O., Zeng, L., Wang, S., 2020. Development of a novel lateral flow biosensor combined with aptamer-based isolation: application for rapid detection of grouper nervous necrosis. Virus 11 (886).
Liu, J., Zeng, J., Tian, Y., Zhou, N., 2018. An aptamer and functionalized nanoparticle-based strip biosensor for on-site detection of kanamycin in food samples. Analyst 143 (1), 182–189.
Mao, X., Ma, Y., Zhang, A., Zhang, L., Zeng, L., Liu, G., 2009. Disposable nucleic acid biosensors based on gold nanoparticle probes and lateral flow strip. Anal. Chem. 81 (4), 1660–1668.
Minagawa, H., Onodera, K., Fujita, H., Sakamoto, T., Akitomi, J., Kaneko, N., Shiratori, I., Kuwahara, M., Horii, K., Waga, I., 2017. Selection, characterization and application of artificial DNA aptamer containing appended bases with sub-nanomolar affinity for a salivary biomarker. Sci. Rep. 7.
Mukama, O., Wu, W., Wu, J., Lu, X., Liu, Y., Liu, Y., Liu, J., Zeng, L., 2020. A highly sensitive and specific lateral flow aptasensor for the detection of human osteopontin. Talanta 210.
Orooji, Y., Sohrabi, H., Hemmat, N., Oroojalian, F., Baradaran, B., Mokhtarzadeh, A., Mohaghegh, M., Karimi-Maleh, H., 2020. An overview on SARS-CoV-2 (COVID-19) and other human coronaviruses and their detection capability via amplification assay, chemical sensing, biosensing, immunosensing, and clinical assays. Nano-Micro Lett. 13 (1).
Ozalp, V.C., Bayramoglu, G., Erdem, Z., Arica, M.Y., 2015. Pathogen detection in complex samples by quartz crystal microbalance sensor coupled to aptamer functionalized core-shell type magnetic separation. Anal. Chim. Acta 853, 533–540.
Quesada-Gonzalez, D., Merkoci, A., 2015. Nanoparticle-based lateral flow biosensors. Biosens. Bioelectron. 73, 47–63.
Ranganathan, V., Srinivasan, S., Singh, A., DeRosa, M.C., 2020. An aptamer-based colorimetric lateral flow assay for the detection of human epidermal growth factor receptor 2 (HER2). Anal. Biochem. 588.
Rasoulinejad, S., Gargari, S.L.M., 2016. Aptamer-nanobody based ELASA for specific detection of Acinetobacter baumannii isolates. J. Biotechnol. 231, 46–54.
Raston, N.H.A., Gu, M.B., 2015. Highly amplified detection of visceral adipose tissue-derived serpin (vaspin) using a cognate aptamer duo. Biosens. Bioelectron. 70, 261–267.
Raston, N.H.A., Van-Thuan, N., Gu, M.B., 2017. A new lateral flow strip assay (LFSA) using a pair of aptamers for the detection of Vaspin. Biosens. Bioelectron. 93, 21–25.
Reid, R., Chatterjee, B., Das, S.J., Ghosh, S., Sharma, T.K., 2020. Application of aptamers as molecular recognition elements in lateral flow assays. Anal. Biochem. 593.
Reinemann, C., von Fritsch, U.F., Rudolph, S., Strehlitz, B., 2016. Generation and characterization of quinolone-specific DNA aptamers suitable for water monitoring. Biosens. Bioelectron. 77, 1039–1047.
Salek Maghsoudi, A., Hassani, S., Rezaei Akmal, M., Ganjali, M.R., Mirnia, K., Norouzi, P., Abdollahi, M., 2020. An electrochemical aptasensor platform based on flower-like gold microstructure-modified screen-printed carbon electrode for detection of serpin A12 as a type 2 diabetes biomarker. Int. J. Nanomed. 15, 2219–2230.
Schüling, T., Eilers, A., Scheper, T., Walter, J., 2018. Aptamer-based lateral flow assays. AIMS Bioengineering 5, 78–102.
Seok, Y., Byun, J.-Y., Shim, W.-B., Kim, M.-G., 2015. A structure-switchable aptasensor for aflatoxin B1 detection based on assembly of an aptamer/split DNAzyme. Anal. Chim. Acta 886, 182–187.
Shim, W.-B., Kim, M.J., Mun, H., Kim, M.-G., 2014. An aptamer-based dipstick assay for the rapid and simple detection of aflatoxin B1. Biosens. Bioelectron. 62, 288–294.
Shin, W.-R., Sekhon, S.S., Rhee, S.-K., Ko, J.H., Ahn, J.-Y., Min, J., Kim, Y.-H., 2018. Aptamer-based paper strip sensor for detecting Vibrio fischeri. ACS Comb. Sci. 20 (5), 261–268.
Soh, J.H., Chan, H.-M., Ying, J.Y., 2020. Strategies for developing sensitive and specific nanoparticle-based lateral flow assays as point-of-care diagnostic device. Nano Today 30.
Sun, J., Gan, Y., Kong, L., Zhou, S., Liang, T., Wang, X., Wan, H., Wang, P., 2019. A novel lateral flow strip based on DNA-functionalized gold nanoparticles for on-site detection of mercury (II) ions. 2019. IEEE International Symposium on Olfaction and Electronic Nose (ISOEN) 1–3.
Sun, S., Zheng, P., Zhao, S., Liu, H., Wang, Z., Peng, T., Wang, J., Yao, K., Wang, S., Zeng, Y., Jiang, H., 2018. Time-resolved fluorescent immunochromatographic assay-based on three antibody labels for the simultaneous detection of aflatoxin B-1 and zearalenone in Chinese herbal medicines. Food Addit. Contam. Part a-Chemistry Analysis Control Exposure & Risk Assessment 35 (12), 2434–2442.
Tasbasi, B.B., Guner, B.C., Sudagidan, M., Ucak, S., Kavruk, M., Ozalp, V.C., 2019. Label-free lateral flow assay for Listeria monocytogenes by aptamer-gated release of signal molecules. Anal. Biochem. 587.
Tripathi, P., Kumar, A., Sachan, M., Gupta, S., Nara, S., 2020. Aptamer-gold nanozyme based competitive lateral flow assay for rapid detection of CA125 in human serum. Biosens. Bioelectron. 165.
Van-Thuan, N., Kwon, Y.S., Gu, M.B., 2017. Aptamer-based environmental biosensors for small molecule contaminants. Curr. Opin. Biotechnol. 45, 15–23.
Van-Thuan, N., Song, S., Park, S., Joo, C., 2020. Recent advances in high-sensitivity detection methods for paper-based lateral-flow assay. Biosens. Bioelectron. 152.
Velu, R., DeRosa, M.C., 2018. Lateral flow assays for Ochratoxin A using metal nanoparticles: comparison of "adsorption-desorption" approach to linkage inversion assembled nano-aptasensors (LIANA). Analyst 143 (19).
Verma, N., Patel, D., Pandya, A., 2020. Emerging diagnostic tools for detection of COVID-19 and perspective. Biomed. Microdevices 22 (4).
Wang, C., Sun, L., Zhao, Q., 2019. A simple aptamer molecular beacon assay for rapid detection of aflatoxin B1. Chin. Chem. Lett. 30 (5), 1017–1020.
Wang, K., Qin, W., Hou, Y., Xiao, K., Yan, W., 2016. The application of lateral flow immunoassay in point of care testing: a review. Nano Biomedicine and Engineering 8.
Wang, L., Ma, W., Chen, W., Liu, L., Ma, W., Zhu, Y., Xu, L., Kuang, H., Xu, C., 2011. An aptamer-based chromatographic strip assay for sensitive toxin semi-quantitative detection. Biosens. Bioelectron. 26 (6), 3059–3062.
Wu, K., Ma, C., Zhao, H., Chen, M., Deng, Z., 2019. Sensitive aptamer-based fluorescene assay for ochratoxin A based on RNase H signal amplification. Food Chem. 277, 273–278.
Wu, S., Liu, L., Duan, N., Li, Q., Zhou, Y., Wang, Z., 2018a. Aptamer-based lateral flow test strip for rapid detection of zearalenone in corn samples. J. Agric. Food Chem. 66 (8), 1949–1954.

Wu, S., Liu, L., Duan, N., Wang, W., Yu, Q., Wang, Z., 2018b. A test strip for ochratoxin A based on the use of aptamer-modified fluorescence upconversion nanoparticles. Microchimica Acta 185 (11).
Wu, W., Zhao, S., Mao, Y., Fang, Z., Lu, X., Zeng, L., 2015. A sensitive lateral flow biosensor for Escherichia coli O157:H7 detection based on aptamer mediated strand displacement amplification. Anal. Chim. Acta 861, 62–68.
Wu, Z., He, D., Xu, E., Jiao, A., Chughtai, M.F.J., Jin, Z., 2018c. Rapid detection of beta-conglutin with a novel lateral flow aptasensor assisted by immunomagnetic enrichment and enzyme signal amplification. Food Chem. 269, 375–379.
Xu, H., Mao, X., Zeng, Q., Wang, S., Kawde, A.-N., Liu, G., 2009. Aptamer-functionalized gold nanoparticles as probes in a dry-reagent strip biosensor for protein analysis. Anal. Chem. 81 (2), 669–675.
Yan, W., Wang, K., Xu, H., Huo, X., Jin, Q., Cui, D., 2019. Machine learning approach to enhance the performance of MNP-labeled lateral flow immunoassay. Nano-Micro Lett. 11 (1).
Yang, Z., Yi, C., Lv, S., Sheng, Y., Wen, W., Zhang, X., Wang, S., 2019. Development of a lateral flow strip biosensor based on copper oxide nanoparticles for rapid and sensitive detection of HPV16 DNA. Sensor. Actuator. B Chem. 285, 326–332.
Yin, J., Zhang, A., Dong, C., Ren, J., 2015. An aptamer-based single particle method for sensitive detection of thrombin using fluorescent quantum dots as labeling probes. Talanta 144, 13–19.
Yu, H., Canoura, J., Guntupalli, B., Lou, X., Xiao, Y., 2017. A cooperative-binding split aptamer assay for rapid, specific and ultra-sensitive fluorescence detection of cocaine in saliva. Chem. Sci. 8 (1), 131–141.
Yu, Q., Zhao, Q., Wang, S., Zhao, S., Zhang, S., Yin, Y., Dong, Y., 2020. Development of a lateral flow aptamer assay strip for facile identification of theranostic exosomes isolated from human lung carcinoma cells. Anal. Biochem. 594.
Zhan, N., Zhou, Y., Mei, L., Han, Y., Zhang, H., 2019. Dual detection of procalcitonin and C-reactive protein with an up-converting nanoparticle based lateral flow assay. Anal. Sci. 35 (3), 257–263.
Zhang, D., Huang, L., Liu, B., Ni, H., Sun, L., Su, E., Chen, H., Gu, Z., Zhao, X., 2018a. Quantitative and ultrasensitive detection of multiplex cardiac biomarkers in lateral flow assay with core-shell SERS nanotags. Biosens. Bioelectron. 106, 204–211.
Zhang, G., Zhu, C., Huang, Y., Yan, J., Chen, A., 2018b. A lateral flow strip based aptasensor for detection of ochratoxin A in corn samples. Molecules 23 (2).
Zhao, S., Wang, S., Zhang, S., Liu, J., Dong, Y., 2018. State of the art: lateral flow assay (LFA) biosensor for on-site rapid detection. Chin. Chem. Lett. 29 (11), 1567–1577.
Zhao, Z., Wang, H., Zhai, W., Feng, X., Fan, X., Chen, A., Wang, M., 2020. A lateral flow strip based on a truncated aptamer-complementary strand for detection of type-B Aflatoxins in Nuts and Dried Figs, 12, p. 136, 2.
Zheng, W., Yao, L., Teng, J., Yan, C., Qin, P., Liu, G., Chen, W., 2018. Lateral flow test for visual detection of multiple MicroRNAs. Sensor. Actuator. B Chem. 264, 320–326.
Zhou, W., Kong, W., Dou, X., Zhao, M., Ouyang, Z., Yang, M., 2016. An aptamer based lateral flow strip for on-site rapid detection of ochratoxin A in Astragalus membranaceus. Journal of Chromatography B-Analytical Technologies in the Biomedical and Life Sciences 1022, 102–108.
Zhu, C., Zhang, G., Huang, Y., Yang, S., Ren, S., Gao, Z., Chen, A., 2018. Dual-competitive lateral flow aptasensor for detection of aflatoxin B-1 in food and feedstuffs. J. Hazard Mater. 344, 249–257.